Supporting Information:

1. Cluster Balance Equations for Nucleation Potential Model

Full cluster balances are given in Equation S1 for the Nucleation Potential Model (NPM). Cluster balances contain formation and loss terms for the various cluster types. Clusters are formed by collisions and lost via coagulation with larger clusters and diffusion to the walls of the flow reactor. Forward rate constants are assumed to be equal with the $k = 4.2 \times 10^{-10}$ cm^3 s^{-1} based on an ideal solution where partial volumes of each component are independent of the liquid composition (Ortega et al., 2012). The forward rate constant is assumed equal across all clusters due to the minimal changes in the rate constant from the smallest cluster to the largest cluster. Cluster size, mass, and dipole moment all impact *k*, sometimes in opposing ways, and these parameters have not been measured for the vast majority of freshly formed clusters. Furthermore, any inaccuracies in the reaction constant will be captured by $[B_{eff}]$. In other words, if the reaction constant is higher than the used value, this will lead to an increase in $[B_{eff}]$. The wall loss rate constant, k_d, is calculated from the diffusion constant of each cluster and a diameter of the reactor (5 cm). k_d ranges from 0.05 s^{-1} to 0.045 s^{-1} for monomer to tetramer, respectively (Froyd and Lovejoy, 2003). The final concentration of particles is the combined concentration of tetramers ($[N_4]$) and larger particles ($[N_{>4}]$).

For the steady-state case of the model, which was applied to atmospheric data, cluster balances up to $[N_3]$ are set equal to zero, and $\frac{d[N_4]}{dt}$ is set equal to the calculated nucleation rate (J_{1nm}). Additionally, wall loss rates are replaced with a coagulation loss rates to pre-existing particles. The coagulation loss rate was calculated from the Fuch's surface area (Kuang et al., 2010) during the various field campaigns and was assumed to be constant over the course of the nucleation events (Sihto et al., 2006; Iida et al., 2008; McMurry and Eisele, 2005; Cai et al., 2021; Eisele et al., 2006).

$$\frac{d[A_1]}{dt} = -k[A_1]\left[B_{eff}\right] - k_d[N_1]$$

$$\frac{d\left[B_{eff}\right]}{dt} = -k[A_1]\left[B_{eff}\right] - k_d[N_1]$$

$$\frac{d\left[A_1 \cdot B_{eff}\right]}{dt} = k[A_1]\left[B_{eff}\right] - k[N_1](2[N_1] + [N_2] + [N_3] + [N_4]) - k_d[N_1]$$

$$[N_1] = \left[A_1 \cdot B_{eff}\right]$$

$$\frac{d[N_2]}{dt} = k[N_1]^2 - k[N_2]([N_1] + 2[N_2] + [N_3] + [N_4]) - k_d[N_2]$$

$$\frac{d[N_3]}{dt} = k[N_1][N_2] - k[N_3]([N_1] + [N_2] + 2[N_3] + [N_4]) - k_d[N_3]$$

$$\frac{d[N_4]}{dt} = k_1[N_2]^2 + k_1[N_1][N_3] - k_1[N_4]([N_1] + [N_2] + [N_3] + 2[N_4]) - k_d[N_4]$$

$$\frac{d[N_{4,+}]}{dt} = k_1[N_1][N_4] + k_1[N_2][N_3] + k_1[N_2][N_4] + k_1[N_2][N_4] + k_1[N_3]^2 + k_1[N_3][N_4] + k_1[N_4]^2 - k_d[N_4]$$

$$J_{1nm} = \frac{d[N_4]}{dt} + \frac{d[N_{>4}]}{dt}$$

Equation S1

2. Methodology to Evaluate the Nucleation Potential Model

As seen in Figure S1, the first set of bars shows a high concentration of particles of $2x10^5$ cm^{-3} at the 1-nm 50% cut-point (d_{50}), ($T_{conditioner}$ = 1 ºC, $T_{initiator}$ = 99 ºC) and a lower concentration of particles of $8x10^4$ cm^{-3} at the 2-nm cut-point, ($T_{conditioner}$ = 2 ºC, $T_{initiator}$ = 90 ºC) when $[A_1]_o = 5x10^9$ cm^{-3}. The second set of bars shows a significantly lower particle concentration of $8x10^3$ cm^{-3} at the 1-nm cut-point and a particle concentration of 30 cm^{-3} at the 2-nm cut-point when $[A_1]_o = 4x10^8$ cm^{-3}. Low concentrations of 2-nm particles in the second set of bars suggests that most formed particles are less than 2 nm in diameter. This inferred size distribution is more compatible with the nucleation model, which accounts for particles up to N_8 (larger than 1 nm). At higher concentrations of $[A_1]_o$, the particle concentrations at the 1-nm cut-point and 2-nm cut-point are not significantly different, indicating that a majority of the particles are larger than 2 nm in diameter. In addition, the high particle concentration (>10^5 cm^{-3}) at high $[A_1]_o$ approaches the upper detection limit of the vwCPC which also increases measurement uncertainty. Note, Scanning Mobility Particle Sizers (SMPS) scans have not been taken for the flow tube due to the large uncertainty associated with charging particles in the 1-nm size range (Jen et al., 2015; Jiang et al., 2011). Future work will explore electrically neutral, size-resolved measurements to further increase the accuracy of NPM in estimating coagulation loss rates.

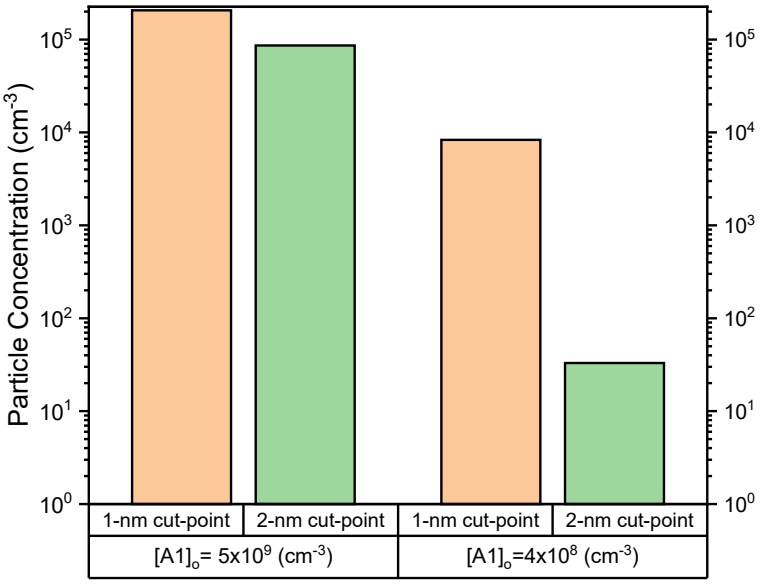

Figure S1: Comparison of particle concentrations at 1-nm and 2-nm d_{50} cut-points for the vwCPC at $[A_1]_o$ =$5x10^9$ cm^{-3} (left) and at $[A_1]_o$ =$4x10^8$ cm^{-3} (right).

References:

Cai, R., Yan, C., Yang, D., Yin, R., Lu, Y., Deng, C., Fu, Y., Ruan, J., Li, X., Kontkanen, J., Zhang, Q., Kangasluoma, J., Ma, Y., Hao, J., Worsnop, D. R., Bianchi, F., Paasonen, P., Kerminen, V.-M., Liu, Y., Wang, L., Zheng, J., Kulmala, M., and Jiang, J.: Sulfuric acid–amine nucleation in urban Beijing, Atmospheric Chem. Phys., 21, 2457–2468, https://doi.org/10.5194/acp-21-2457-2021, 2021.

Eisele, F. L., Lovejoy, E. R., Kosciuch, E., Moore, K. F., Mauldin, R. L., Smith, J. N., McMurry, P. H., and Iida, K.: Negative atmospheric ions and their potential role in ion-induced nucleation, J. Geophys. Res. Atmospheres, 111, https://doi.org/10.1029/2005JD006568, 2006.

Fomete, S. K. W., Johnson, J. S., Casalnuovo, D., and Jen, C. N.: A tutorial guide on new particle formation experiments using a laminar flow reactor, J. Aerosol Sci., 157, 105808, https://doi.org/10.1016/j.jaerosci.2021.105808, 2021.

Froyd, K. D. and Lovejoy, E. R.: Experimental Thermodynamics of Cluster Ions Composed of H2SO4 and H2O. 1. Positive Ions, J. Phys. Chem. A, 107, 9800–9811, https://doi.org/10.1021/jp027803o, 2003.

Hanson, D. R., Burkholder, J. B., Howard, C. J., and Ravishankara, A. R.: Measurement of hydroxyl and hydroperoxy radical uptake coefficients on water and sulfuric acid surfaces, J. Phys. Chem., 96, 4979–4985, https://doi.org/10.1021/j100191a046, 1992.

Hanson, D. R., Bier, I., Panta, B., Jen, C. N., and McMurry, P. H.: Computational Fluid Dynamics Studies of a Flow Reactor: Free Energies of Clusters of Sulfuric Acid with NH3 or Dimethyl Amine, J. Phys. Chem. A, 121, 3976–3990, https://doi.org/10.1021/acs.jpca.7b00252, 2017.

Iida, K., Stolzenburg, M. R., McMurry, P. H., and Smith, J. N.: Estimating nanoparticle growth rates from size-dependent charged fractions: Analysis of new particle formation events in Mexico City, J. Geophys. Res. Atmospheres, 113, https://doi.org/10.1029/2007JD009260, 2008.

Jen, C. N., Hanson, D. R., and McMurry, P. H.: Towards Reconciling Measurements of Atmospherically Relevant Clusters by Chemical Ionization Mass Spectrometry and Mobility Classification/Vapor Condensation, Aerosol Sci. Technol. ARL, 49, i–iii, https://doi.org/10.1080/02786826.2014.1002602, 2015.

Jiang, J., Chen, M., Kuang, C., Attoui, M., and McMurry, P. H.: Electrical Mobility Spectrometer Using a Diethylene Glycol Condensation Particle Counter for Measurement of Aerosol Size Distributions Down to 1 nm, Aerosol Sci. Technol., 45, 510–521, https://doi.org/10.1080/02786826.2010.547538, 2011.

Kuang, C., Riipinen, I., Sihto, S. L., Kulmala, M., McCormick, A. V., and McMurry, P. H.: An improved criterion for new particle formation in diverse atmospheric environments, Atmos Chem Phys, 10, 8469–8480, https://doi.org/10.5194/acp-10-8469-2010, 2010.

McMurry, P. H. and Eisele, F. L.: Preface to topical collection on new particle formation in Atlanta, J. Geophys. Res. Atmospheres, 110, https://doi.org/10.1029/2005JD006644, 2005.

Murphy, D. M. and Fahey, D. W.: Mathematical treatment of the wall loss of a trace species in denuder and catalytic converter tubes, Anal. Chem., 59, 2753–2759, https://doi.org/10.1021/ac00150a006, 1987.

Ortega, I. K., Kupiainen, O., Kurtén, T., Olenius, T., Wilkman, O., McGrath, M. J., Loukonen, V., and Vehkamäki, H.: From quantum chemical formation free energies to evaporation rates, Atmospheric Chem. Phys., 12, 225–235, https://doi.org/10.5194/acp-12-225-2012, 2012.

Panta, B., Glasoe, W. A., Zollner, J. H., Carlson, K. K., and Hanson, D. R.: Computational Fluid Dynamics of a Cylindrical Nucleation Flow Reactor with Detailed Cluster Thermodynamics, J. Phys. Chem. A, 116, 10122–10134, https://doi.org/10.1021/jp302444y, 2012.

Pöschl, U., Canagaratna, M., Jayne, J. T., Molina, L. T., Worsnop, D. R., Kolb, C. E., and Molina, M. J.: Mass Accommodation Coefficient of H2SO4 Vapor on Aqueous Sulfuric Acid Surfaces and Gaseous Diffusion Coefficient of H2SO4 in N2/H2O, J. Phys. Chem. A, 102, 10082–10089, https://doi.org/10.1021/jp982809s, 1998.

Sihto, S. L., Kulmala, M., Kerminen, V. M., Dal Maso, M., Petäjä, T., Riipinen, I., Korhonen, H., Arnold, F., Janson, R., Boy, M., Laaksonen, A., and Lehtinen, K. E. J.: Atmospheric sulphuric acid and aerosol formation: implications from atmospheric measurements for nucleation and early growth mechanisms, Atmos Chem Phys, 6, 4079–4091, https://doi.org/10.5194/acp-6-4079-2006, 2006.